"DMD #4713

# METABOLISM, EXCRETION AND PHARMACOKINETICS OF (3-{[4-*TERT*-BUTYL-BENZYL)-(PYRIDINE-3-SULFONYL)-AMINO]-METHYL}-PHENOXY)-ACETIC ACID, AN EP-2 RECEPTOR SELECTIVE PGE2 AGONIST, IN MALE AND FEMALE SPRAGUE-DAWLEY RATS

KIM A JOHNSON AND CHANDRA PRAKASH

Department of Pharmacokinetics, Dynamics and Metabolism, Pfizer Global Research and Development, Groton, Connecticut

1

# BIOTRANSFORMATION OF A PYRIDINYL SULFONAMIDE ANALOG

[1]Abbreviations used are: PGE2, prostaglandin E2; i.v., intravenous; SD; Sprague-Dawley; LSC, liquid scintillation counting; LC/MS/MS, liquid chromatography-tandem mass spectrometry; HPLC, high performance liquid chromatography; radio-HPLC, HPLC with on-line radioactivity detection; ARC, accurate radioisotope counting; RAM, radioactivity monitor; $T_{1/2}$, terminal phase half-life; $AUC_{0-T}$, area under the plasma concentration-time curve from time 0 to T; $CL_p$, systemic plasma clearance; $VD_{ss}$, steady-state volume of distribution; CID, Collision induced dissociation; MS, mass spectrometry

Address for Correspondence:

Chandra Prakash, Ph. D.
Pharmacokinetics, Dynamics and Metabolism
Pfizer Global Research and Development
Groton, CT 06340
Ph. No. 860-441-6415
Fax No. 860-441-4109
email: Chandra_prakash@groton.pfizer.com

Text pages    35

Tables        5

Figures       11

References     22

Abstract      246

Introduction  377

Discussion    1029

ABSTRACT

Metabolism, excretion and pharmacokinetics of a highly selective EP2 agonist, CP-533,536; (3-{[4-*tert*-butyl-benzyl)-(pyridine-3-sulfonyl)-amino]-methyl}-phenoxy)-acetic acid), were investigated in male and female Sprague-Dawley rats following an intravenous administration of a single 15 mg/kg dose of [$^{14}$C]CP-533,536. At 144 h after the dose, the cumulative excretion of radioactivity averaged 98.2±3.44% and 97.0±4.82% in male and female rats, respectively. The radioactivity was predominantly excreted in feces, reaching 87% of the dose. Mean exposure (AUC$_{0-\infty}$) for both CP-533,536 and total radioactivity was higher in female rats than male rats, while the plasma clearance of CP-533,536 and metabolites was lower in female rats compared to male rats. CP-533,536 was extensively metabolized in both male and female rats. The major oxidative pathway was due to the oxidation of the *tert*-butyl side chain to form the ω-hydroxy metabolite M4 (males, 19.7%; females 6.5%). M4 was further oxidized to form the ω-carboxy metabolite M3 (males, 32.8%; females 1.66%) or conjugated via sulfation to form metabolite M6 (males 12.7%; females 36.2%). Other metabolites were due to N-oxidation of the pyridine ring (M5) and aromatic hydroxylation (M12), and conjugation with glucuronic acid. The secondary metabolites were due to N-dealkylation of the methyl-phenoxyacetic acid moiety and phase II conjugation. CP-536,536 accounted for about 63 and 72% of the AUC of the total radioactivity for male and female rats, respectively. Gender-related differences in the metabolism and pharmacokinetics were observed. ω-

**"DMD #4713**

Carboxy metabolite M3 was the major metabolite in male rats, whereas M3-sulfate was identified as the major metabolite in female rats.

"DMD #4713

Approximately 8 million bone fractures occur annually in the United States (Melton, 1995). Most of these cause interruption of work and activities of daily life, and many are associated with long-term or permanent disability. PGE2[1] has been shown to significantly increase bone mass and bone strength when administered systemically or locally to the skeleton (Jee and Ma, 1997 and Ke et al., 1998). However, due to severe side effects including diarrhea, lethargy, and flushing, PGE2 is an unacceptable therapeutic option (Jee and Ma 1997). The action of PGE2 is mediated by 4 distinct receptor subtypes: EP1, EP2, EP3, and EP4 (Breyer et al., 2001). Two of the subtypes, EP2 and EP4, signal via a cAMP pathway and are involved in mediating bone anabolic effect of PGE2. It has been shown that EP2-selective agonists, when delivered locally to the periosteal surface or the marrow cavity of bones, increase cortical and cancellous bone formation without the systemic side effects observed with PGE2 (Breyer et al., 2001).

CP-533,536; (3-{[(4-*tert*-butyl-benzyl)-(pyridine-3-sulfonyl)-amino]-methyl}-phenoxy)-acetic acid (Fig. 1) is a highly selective and potent functional EP2 receptor agonist. (Paralkar et al., 2003). In *in vivo* studies, CP-533,536 stimulated local bone formation when injected onto the periosteal surface and into the marrow cavity of long bones in rat models. In addition, CP-533,536 enhanced bone healing in rat and dog fracture models. Furthermore, CP-533,536 induced new bone formation and healed critical-sized segmental defects

of long bones in the dog (Paralkar et al., 2003). Therefore, CP-533,536 offers a promising therapeutic alternative for the enhancement of bone healing and treatment of bone defects and fractures in humans.

Preclinical pharmacokinetic studies of CP-533,536 in rats, monkey and dogs following an i.v. administration suggested that it is extensively metabolized. In each species, the plasma levels of unchanged CP-533,536 declined with a short $T_{1/2}$, suggesting rapid elimination of CP-533,536 (Plowchalk et al., unpublished work). The objectives of the present study were to characterize metabolism, pharmacokinetics and excretion of [$^{14}$C]CP-533,536 in SD rats as part of the preclinical development of this EP-2 receptor antagonist. The metabolites were characterized by LC/MS/MS and the isomeric structures were differentiated by chemical derivatization techniques. The structures of metabolites, where possible, were supported by comparisons of their retention times on HPLC, and MS spectra with those of synthetic standards.

## Materials and Methods

**General Chemicals**. Commercially obtained chemicals and solvents were of HPLC or analytical grade. β-Glucuronidase (from Helix Pomatia, type H-1 with sulfatase activity) was obtained from Sigma Chemical Company (St. Louis, MO). YMC AQ (C-18) analytical and preparative columns were obtained from YMC (Wilmington, NC). Ecolite (+) scintillation cocktail was obtained from ICN (Irvine, CA). Carbosorb and Permafluor E+ scintillation cocktails were purchased from Packard Instrument Company (Downers Grove, IL). HPLC grade acetonitrile,

methanol, water, certified ACS grade ammonium acetate, acetic acid and aqueous titanium chloride (20%) were obtained from J. T. Baker (Phillipsburg, NJ).

**Radiolabelled Drug and Reference Compounds.** [$^{14}$C]CP-533,536, specific activity 4.36 mCi/mmol (Fig. 1), was synthesized by the Radiosynthesis Group at Pfizer Global Research and Development (Groton, CT).  It showed a radiochemical purity of ≥98%, as determined by radio-HPLC.  The synthetic reference standards, ω-carboxy-, (M3; 2-(4-{[(3-carboxymethoxy-benzyl)-(pyridine-3-sulfonyl)-amino]-methyl}-phenyl)-2-methyl-propionic acid) and ω-hydroxy-, (M4; (3-{[[4-(2-hydroxy-1,1-dimethyl-ethyl)-benzyl]-(pyridine-3-sulfonyl)-amino]-methyl}-phenoxy)-acetic acid) were synthesized by the Medicinal Chemistry Group at Pfizer Global Research and Development (Groton, CT).

**Animal Studies.**  Bile-duct and/or jugular-vein cannulated SD rats (190-270 g) were purchased from Charles River Laboratories (Stoneridge, NY).  Animals were quarantined for a minimum of 3 days prior to treatment and maintained on a 12-h light/dark cycle. The animals were housed individually in stainless steel metabolism cages.  The rats were fasted overnight prior to administration of the dose and were fed 6 h after the dose.  The animals were provided water *ad libitium*.  All studies were conducted in a research facility accredited by the American Association for the Accreditation of Laboratory Animal Care.

*Metabolism and excretion studies.* A group of three male and three female jugular vein cannulated SD rats received a single 15 mg/kg i.v. dose of [$^{14}$C]CP-533,536 via jugular vein.  Urine and feces were collected at -18 to 0 h pre-dose and at 24-h intervals for the seven consecutive days after dose administration. Urine was collected into containers surrounded by ice.  Feces were frozen immediately at the end of each collection interval.  Urine and feces were stored frozen at approximately -20 $^{o}$C until analysis.

*Pharmacokinetics.* A second group of three male and three female jugular vein cannulated SD rats were administered a single 15 mg/kg i.v. dose of [$^{14}$C]CP-533,536.  Whole blood (approximately 0.6 ml) was collected from jugular vein into heparinized tubes at 5, and 15 min, and 1, 2, 4, 6, 8, 24, and 48 h after administration of the dose.  All animals were sacrificed by exsanguination 48 h after dosing.  For circulating metabolites identification, a third group of two male and two female SD rats were administered a single 15 mg/kg i.v. dose of [$^{14}$C]CP-533,536.  Whole blood (approximately 2 ml) was collected from jugular vein into heparinized tubes at 1 and 4 h post dose. Plasma was separated from whole blood by centrifugation. The plasma was stored frozen at approximately -20 $^{o}$C until analysis for radioactivity and CP-533,536 concentrations.

*Bile duct-cannulated study.*  Two male and two female bile duct and jugular-vein cannulated SD rats were administered a single 15 mg/kg i.v. dose of [$^{14}$C]CP-

533,536.  Bile was collected at 0-8 h post-dose.  The samples were stored frozen at approximately -20 $^o$C until analysis.

**Determination of Radioactivity.**  The radioactivity in urine, bile and plasma was determined by LSC.  Aliquots of urine (0.1 g), bile (0.025 g) or plasma (0.025 g) were mixed with 5 ml of Ecolite (+) scintillation cocktail and counted in a Wallac #1409 liquid scintillation counter (Gaithersburg, MD).  Fecal samples were mixed with equal amounts of water, and homogenized using a Stomacher homogenizer (Cooke Laboratory Products, Alexandria, VA).  , Triplicate aliquots (0.1-0.3 g) of each fecal homogenate were combusted using a model 307 oxidizer (Packard, Downers Glove, IL) and the radioactivity in the combustion products was determined as described earlier (Johnson et al., 2003).  Radioactivity less than twice the background value was considered to be below the limit of determination.  The samples collected prior to dosing were used as controls and counted to obtain background count rate.

The radioactivity in the dose was established as 100% of the total radioactivity. The radioactivity at each sampling time for urine and feces was defined as the percentage of dose excreted in the respective matrices. The radioactivity measured in plasma was converted to ng-equiv of CP-533,536 based on the specific activity of the dose (19.75 dpm/ng).

**Extraction of Metabolites from Biological Samples**.  Urine samples (~10 ml, 0-24 h) were evaporated under nitrogen gas in a Turbo Vap LV evaporator

(Zymark, Hopkinton, MA). Sample residues were reconstituted in 1 ml of 0.1% formic acid/acetonitrile (50:50). These solutions were vortexed for about 1 min, transferred to 1.5 ml eppendorf tubes and then centrifuged at 14,000 rpm for about 2 min. Aliquots (10-20 µl) of the supernatants were injected onto the HPLC column without further purification.

Fecal homogenates containing the highest levels of excreted radioactivity (0-48 h) were pooled. From the pooled samples (~80-135 g), aliquots (~5 g) were suspended in 15 ml of acetonitrile. Suspensions were sonicated (~30 min.), vortexed and centrifuged at 3200 rpm for 10 min. Following supernatant transfer to clean 15 ml conical tubes, the residues were further extracted 2 times with 15 ml of acetonitrile as described above. Aliquots (200 µl) from each extraction were counted in a liquid scintillation counter. The recovery of radioactivity ranged from 92-96%. The supernatants were evaporated to dryness under nitrogen in a Turbo Vap LV evaporator (Zymark, Hopkinton, MA) and the residues were reconstituted in 2 ml of mobile phase. Aliquots (10-20 µl) of concentrated fecal extracts were injected onto the HPLC column.

For the identification of circulating metabolites, plasma samples collected at 1 and 4 h for each gender were pooled. The pooled plasma (~ 5 ml) was precipitated using 2 volumes of acetonitrile. The suspensions were sonicated (~30 min), vortexed and centrifuged at 3200 rpm for 10 min. Following supernatant transfer to clean 15 ml conical tubes, the residues were further extracted with 2x15 ml of acetonitrile as described above. The supernatants

were combined and aliquots (500 µl) were counted in a liquid scintillation counter.

The recovery of radioactivity extracted ranged from 85-92%. The solvents were

evaporated to dryness under nitrogen in a Turbo Vap LV evaporator (Zymark,

Hopkinton, MA) and the residues were reconstituted in 0.5 ml of mobile phase.

Aliquots (50-100 µl) of concentrated plasma extracts were injected onto the

HPLC column.

Bile (20-50 µl) was directly injected into the HPLC/MS system for analysis without

further purification.

**HPLC.** The HPLC system consisted of a HP-1100 solvent delivery system, a

HP-1100 membrane degasser, an HP-1100 autoinjector (Hewlett Packard, Palo

Alto, CA) and a radioactive monitor ($\beta$-RAM; IN/US, Tampa, FL).

Chromatography was performed on a YMC AQ $C_{18}$ column (4.6 mm x 150 mm, 3

µm) with a mobile phase containing a mixture of 10 mM ammonium formate pH

5.0 (solvent A) and acetonitrile (solvent B). The mobile phase was initially

composed of solvent A/solvent B (90:10), and held for 3 min. The mobile phase

composition was then linearly programmed to solvent A/solvent B (35:65), over

22 min. A short gradient was programmed to solvent A/solvent B (10:90) over 1

min and these conditions were held for 3 min. The mobile phase composition

was returned to the starting solvent mixture over 3 min. The system was allowed

to equilibrate for 10 min prior to the next injection. A flow rate of 1.0 ml/min was

used for all analyses.

**Quantitative Assessment of Metabolites**. Quantification of the metabolites was carried out by measuring radioactivity in the individual HPLC-separated peaks using a β-RAM. The β-RAM provided an integrated printout in counts per minute and percentage of the radiolabelled material, as well as peak representation. The β-RAM was operated in the homogeneous liquid scintillation counting mode, with addition of 3 ml/min of Tru-Count scintillation cocktail to the effluent after UV detection. For the quantification of plasma metabolites, the HPLC effluent was directed into the flow cell of a β-RAM radioactivity detector. The β-RAM and HPLC were controlled externally using an ARC system (AIM Research; Newark, DE) for low-level radioactivity counting.

**LC-MS/MS**. LC/MS/MS was conducted with a Finnigan TSQ 7000 (Thermo Finnigan, San Jose, CA) equipped with an API-2 electrospray ion source. The effluent from the HPLC column was split, and about 50 µl/min was introduced into the atmospheric ionization source. The remaining effluent was directed to the flow cell of the β-RAM. The β-RAM response was recorded as a real time analog signal by the mass spectrometer data collection system, which provided simultaneous detection of radioactivity and MS data. The electrospray interface was operated at 4500 V, and the mass spectrometer was operated in the positive ion mode. CID studies were performed using argon gas at the collision energy of 30 to 35 eV and at a pressure of approximately 2.1 mTorr. Data were processed with a computer operating ICIS 3.2.1 and Xcalibur 1.3 (Thermo Finnigan, San Jose, CA).

**Quantitation of CP-533,536 in Plasma.** CP-533,536 was quantitated using an LC-MS/MS assay. Aliquots of plasma (25 µl) were pipetted into 96 well plates. 200 µl of 1% acetic acid and 50 µl internal standard (IS) CP-459,310 was added (0.25 mg/ml in 50/50 methanol/water). Extraction of the samples was performed using a Tomtec Quadra 3 (Tomtec; Hamden, CT). Prior to extraction of samples, a Waters Max Oasis (Part# 186000375, Waters; Milford, MA) plate was conditioned with 200-µl methanol, followed by 400 µl of 95% 50 mM sodium acetate pH 7/5% methanol. Plasma samples were applied to the pre-conditioned extraction plate. The plate was washed with 400 µl of 95% 50 mM sodium acetate pH 7/5% methanol followed by 400 µl methanol. Samples were eluted into a deep-well plate with 100 µl methanol containing 2% formic acid. The methanol was evaporated under nitrogen until dryness. Samples were reconstituted in mobile phase (100 µl; 20% 10 mM ammonium acetate and 80% acetonitrile). Samples were quantitated on a PerkinElmer Sciex API-3000 HPLC/MS/MS system (PerkinElmer Sciex Instruments, Boston, MA) using Turbo ion spray source. The ion source was operated at 4500 V, and the mass spectrometer was operated in the negative ion mode. CP-533,536 and IS were separated on a Luna CN column (2.0 x 50 mM, 5 µm particles), at a flow rate of 0.4 ml/min. MRM transitions for the drug and IS were 467→409.3 and 388.1→198.4, respectively. The dynamic range of the assay was from 1 to 5000 ng/ml.

**Data Analysis.** Plasma concentration-time profiles were analyzed using a well established non-compartmental model in WinNonlin v2.1 (Pharsight, Mountain

"DMD #4713

View, CA). Pharmacokinetic parameters were estimated using the methods as described earlier (Johnson et al., 2003). Plasma concentrations below the lower limit of quantitation were treated as 0.0 ng/ml for purposes of calculating mean and standard deviation (SD) of plasma concentrations at each sampling time and for calculating pharmacokinetic parameters. Standard deviations were determined for a time point when at least 50% of values had measurable plasma concentrations.

## Results

**[14]C-Excretion**. After i.v. administration of a single 15 mg/kg dose of [^{14}C]CP-533,536 to rats, radioactivity was excreted predominantly in the feces (Table 1). At 144 h after the dose, the excretion in feces averaged 86.2±1.33% of the administered dose in male rats, and 87.8±3.58% of the dose in female rats. In the urine, 12.0±3.41% and 9.18±1.31% of the administered radioactivity was excreted in male and female rats, respectively. In total, the cumulative excretion of radioactivity averaged to 98.2±3.44% and 97.0±4.82% in male and female rats, respectively. Elimination of the radioactivity was rapid. Of the entire radioactivity recovered in urine and feces of rats >90% was excreted in the first 24 h after dose administration.

**Pharmacokinetics**. Mean plasma concentration versus time curves of CP-533,536 and total radioactivity after a single 15 mg/kg i.v. dose of [^{14}C]CP-

533,536 to rats are shown in fig. 2.  The mean (±SD) plasma concentrations of unchanged CP-533,536 were 20.0±6.47 and 33.1±8.76 µg/ml for male and female rats, respectively, at the first time point (5 min) after administration. Concentrations then declined monoexponentially to <0.1 µg/mL after 8 h.  Mean $AUC(0-\infty)$ values for unchanged CP-533,536 were 9.72±2.80 and 15.6±0.82 µg•h/ml, respectively, in male and female rats (Table 2).  $VD_{ss}$ values were 2.93 and 0.71 l/kg for male and female rats, respectively. The mean $Cl_p$ was modest with a mean value of 30.2 and 16.1 ml/min/kg for male and female rats, respectively.

**Total radioactivity.** The mean (±SD) plasma concentrations for total radioactivity were 20.1±8.65 and 34.5±5.65 µg-equiv/ml for male and female rats, respectively, at the first time point (5 min) after administration (Table 2).  Mean $AUC_{(0-\infty)}$ values for total radioactivity were 15.5±4.44 and 21.5±4.33 µg-equiv•h/ml in male and female rats, respectively.  Based on $AUC_{(0-\infty)}$ values, approximately 63 and 72% of the circulating radioactivity was attributable to the unchanged drug for male and female rats, respectively.

**Metabolic Profiles in Biological samples.** *Urine.* Representative HPLC radio-profiles recorded with an in-line radioactivity detector, for urine from one male and one female rat are shown in fig. 3.  There were notable qualitative and quantitative gender related differences in the urinary metabolites between male and female rats.  A total of two metabolites in male urine and four metabolites in

female urine were detected.   The major metabolites in male rat urine were M8 (2.22% of dose) and M11 (5.66% of dose), whereas the major metabolites in female rat urine were M4 (0.88%), M10 (4.95%) and M11 (1.59%, Table 3).

**Feces**. Representative HPLC radiochromatograms for fecal metabolites from male and female rats are shown in fig. 4.  In addition to unchanged drug, five metabolites in males and four metabolites in females were detected. The major metabolites in male rat were M3 (32.8% of dose), M4 (19.7% of dose) and M6 (12.7% of dose), whereas in female rat feces, the major metabolites were M4 (5.64% of dose), M6 (36.2% of dose) and M10 (7.34% of dose, Table 3).  The unchanged CP-533,536 accounted for 16.2 and 45.6% of the dose in male and female rats, respectively.

**Bile.**   Representative HPLC radiochromatograms for biliary metabolites from male and female rats are shown in fig. 5.   In addition to parent drug, nine metabolites in male bile and five metabolites in female bile were detected.  The major metabolites in male rat bile were M3, M4, M5 and M6, whereas in female rat bile, the major metabolites were M5, M6 and M11 (Table 4).

**Circulating Metabolites.**   Representative HPLC radiochromatograms of circulating metabolites at 4 h samples of male and female rats are shown in fig. 6.   CP-533,536 and three metabolites (M4, M5 and M6) in males and two

metabolites (M4 and M5) in females were identified. There were notable gender-related quantitative differences in the circulating metabolites (Table 4). CP-533,536 accounted for 21% and 65% of total circulating radioactivity at 4 h in male and female rats, respectively (Table 4).

**Identification of the Major Metabolites**

The structures of metabolites were elucidated by electro spray LC/MS/MS using combination of full and product ion scanning techniques (Prakash et al, 1997; 1998; Johnson et al., 2003). The structures of major metabolites, where possible, were supported by comparisons of their retention times on HPLC and MS spectra with those of synthetic standards.

CP-533,536 displayed a protonated molecular ion at *m/z* 469. The product ion mass spectrum of *m/z* 469 showed signals at *m/z* 423, 413, 326, 192, 165, and 147 (Fig. 7). The ion at *m/z* 423 occurred from the loss of formic acid. The diagnostic fragment ion at *m/z* 326 resulted from cleavage of the sulfonamide bond and corresponded to the *tert*-butylbenzyl-methyl-phenoxyacetic moiety. The ion at *m/z* 165 was due to a protonated methyl phenoxyacetic acid moiety, and the ion at *m/z* 147 corresponded to *tert*-butyltropylium ion.

***Metabolite M3.*** M3 had a retention time of ~13.5 min on HPLC and was found in bile (male) and feces. Mass spectral analysis showed a protonated molecular ion at *m/z* 499. The 30-amu increase in molecular weight is in accordance with

oxidation of the methyl group to a carboxyl group. The fragment ions at *m/z* 453, 356, 310, 165 and 131 in its product ion mass spectrum further suggested the oxidation of the methyl group (Table 5). Based on comparison of the HPLC retention time and the CID spectrum with the synthetic standard, M3 was identified as 2-(4-{[(3-carboxymethoxy-benzyl)-(pyridine-3-sulfonyl)-amino]-methyl}-phenyl)-2-methyl-propionic acid.

*Metabolite M4*. M4 had a retention time of ~14.2 min on HPLC and was found in feces, bile, plasma and female rat urine. Its full scan MS displayed a protonated molecular ion at *m/z* 485 (16 amu higher than the parent drug). The product ion mass spectrum of *m/z* 485 showed fragment ions at *m/z* 467, 342, 324, 192, 165, and 145 (Fig. 8). The ion at *m/z* 467, loss of a water molecule from the protonated molecular ion, suggested the presence of an alcoholic group. The ion at *m/z* 145, 2 amu lower than that of the parent drug at m/z 147, suggested that the hydroxylation had occurred at the *tert*-butylbenzyl moiety and a molecule of water had been lost during the fragmentation. Also HPLC retention time of M4 was identical with the retention time of synthetic standard. Thus, M4 was identified as (3-{[[4-(2-hydroxy-1,1-dimethyl-ethyl)-benzyl]-(pyridine-3-sulfonyl)-amino]-methyl}-phenoxy)-acetic acid.

*Metabolite M5*. M5 had a retention time of ~15.4 on HPLC and was found in plasma and bile. Full scan MS of M5 displayed a protonated molecular ion at *m/z* 485 (16 amu higher than the parent drug). CID product ion MS of M5 showed fragment ions at *m/z* 439, 326, 165, and 147 (Fig. 9). The ions at *m/z*

326, 165 and 147 were similar to those of the parent drug, suggesting that the methylphenoxy acetic acid and the *tert*-butylbenzyl moieties were unchanged. Treatment of M5 with aqueous TiCl$_3$ resulted in the formation of CP-533,536. Based on these data, M5 was tentatively identified as (3-{[(4-*tert*-butyl-benzyl)-(pyridine-N-oxide-3-sulfonyl)-amino]-methyl}-phenoxy)-acetic acid.

***Metabolite M6.*** M6 had a retention time of ~12.0 min on HPLC and was found in feces, bile and plasma. MS analysis of M6 showed a protonated molecular ion at *m/z* 565 (96 amu higher than the parent drug), suggesting the addition of an oxygen atom and a sulfate group. The CID product ion MS of M6 showed fragments at *m/z* 485, 467, 342, 324, 165 and 145 (Table 5). The ions at m/z 485 and 467 were due to subsequent losses of the sulfate and water molecules from the protonated molecular ion. The diagnostic ion at *m/z* 145, two amu lower than that of the parent drug, suggested that the hydroxylation had occurred at the *tert*-butylbenzyl moiety and a molecule of water had been lost during the fragmentation. Based on this data, M6 was tentatively identified as the sulfate conjugate of (3-{[[4-(2-hydroxy-1,1-dimethyl-ethyl)-benzyl]-(pyridine-3-sulfonyl)-amino]-methyl}-phenoxy)-acetic acid.

***Metabolite M8.*** M8 had a retention time of ~11.0 min and showed a protonated molecular ion at *m/z* 351,118 amu lower that the parent drug, suggesting that it was a cleaved metabolite. The MS/MS spectrum of M8 gave fragments at *m/z* 305, 146 and 131 (Table 5). The ion at *m/z* 305, loss of 46 amu from the protonated molecular ion, suggested the presence of a carboxylic acid moiety.

The ions at *m/z* 131 and 146 may have resulted from the carboxy-isopropyl benzyl and carboxy isopropyl-benzyl amine moieties, respectively, with the concomitant loss of the formic acid. Based on its fragmentation pattern and molecular ion, it is suggested that M8 was formed from N-debenzylation of the phenoxy acetic acid moiety, followed by oxidation of the methyl group of *tert*-butyl moiety to the carboxylic acid and hydroxylation of the pyridine ring. Reaction of this metabolite with aqueous TiCl₃ caused the retention time of this metabolite to increase by approximately 1 min, and the resulting (M+H)$^+$ ion to decrease by 16 amu, suggesting the presence of an N-oxide. Based on this data, M8 was identified as 2-{4-[pyridine-N-oxide-3-sulfonylamino)-methyl]-phenyl}-2-methyl-propionic acid.

***Metabolite M9***. M9 had a protonated molecular ion at *m/z* 417 and was detected only in female rat urine. The protonated molecular ion at *m/z* 417, 52 amu lower than the parent drug, suggested that the M9 was a cleaved product. The CID product ion spectrum of M9 showed ions at *m/z* 319, 160 and 145 (Table 5). The ion at *m/z* 319, 98 amu lower than the protonated molecular ion, suggested a loss of a molecule of water and sulfate from the molecule. The ion at *m/z* 145, two amu lower than that of the parent drug, suggested that the hydroxylation had occurred on the *tert*-butylbenzyl moiety and a molecule of water had been lost during the fragmentation. Additionally, reaction of this metabolite with TiCl₃ suggested that M9 was an N-oxide. Based on these data, the structure of M9 was proposed as the sulfate conjugate of pyridine-N-oxide-3-sulfonic acid 4-(2-hydroxy-1,1-dimethyl-ethyl)-benzyl amide.

***Metabolite M10***. Full MS of M10 displayed a protonated molecular ion at *m/z* 401, 68 amu lower than the parent drug, suggested that it was a cleaved product. The CID product ion MS of M10 showed fragment ions at *m/z* 303, 160 and 145. The ion at m/z 303, 98 amu lower than the protonated molecular ion, suggested loss of the sulfuric acid from the molecule. The ion at *m/z* 145, 2 amu lower than that of the parent drug at *m/z* 147 (Table 5), suggested that the *tert*-butylbenzyl had been hydroxylated and a molecule of water had been lost during the fragmentation. Based on these data, the structure of M10 was tentatively proposed as the sulfate conjugate of pyridine-3-sulfonic acid 4-(2-hydroxy-1,1-dimethyl-ethyl)-benzyl amide.

***Metabolite M11***. M11 had a retention time of ~12.9 min and was found in urine and bile and showed a protonated molecular ion at *m/z* 335. The molecular ion at *m/z* 335, 134 amu lower than the parent drug, suggested that it was a cleaved product. The CID spectrum of M11 had prominent fragments at *m/z* 289, 146 and 131 (Table 5). The ion at *m/z* 289, a 46 amu loss from the molecular ion, suggested the presence of a carboxylic acid moiety. The ions at *m/z* 131 and 146 may have resulted from the carboxy-isopropyl benzyl and carboxy-isopropyl benzyl amine moieties, respectively, with the concomitant loss of the formic acid. Based on these data, the structure of M11 was tentatively proposed as 2-methyl-2-{4-[(pyridine-3-sulfonylamino)-methyl]-phenyl}-propionic acid.

***Metabolite M12***. M12 had a retention time of ~16.8 min on HPLC and was found in feces and bile. Full scan MS analysis showed a protonated molecular

ion at *m/z* 485 (16 amu higher than the parent drug). The CID product ion MS of

M12 showed prominent fragments at *m/z* 342, 305, 181, 162 and 147 (Fig. 10).

The ions at *m/z* 162 and 147 were similar to those seen in the parent drug,

suggesting that the *tert*-butyl benzyl moiety was unchanged. The ions at *m/z* 181

and 342 were 16 amu higher than those observed in the parent drug (m/z 165

and m/z 326, respectively), indicating the addition of an oxygen atom to the

methylphenoxy acetic acid moiety. The ion at *m/z* 305 was due to loss of the

hydroxy phenoxy acetic acid moiety. Based on these data, M12 was tentatively

identified as (5-{[[(4-tert-butyl-benzyl)-(pyridine-3-sulfonyl)-amino]-methyl}-

hydroxy-phenoxy)-acetic acid.

***Metabolite M13***. M13 had a retention time of ~10.8 (min on HPLC and was

detected only in bile (males). Full scan MS of M13 showed a protonated

molecular ion at *m/z* 561. The CID product ion MS of M13 gave fragment ions at

*m/z* 485, 467, 342, 324, 165, and 145 (Table 5). The ion at *m/z* 485, loss of 176

mass units, suggested the presence of a glucuronide moiety. The ion at *m/z* 467

occurred from the loss of water from the ion at *m/z* 485. The ions at *m/z* 342 and

324 resulted from the subsequent losses of a sulfonyl pyridine moiety and water.

The ion at *m/z* 165, similar to that of the parent drug, was due to a protonated

methyl phenoxy acetic acid moiety. Treatment of M13 with β-glucuronidase

resulted in the formation of M4. Based on these data, M13 was tentatively

identified as glucuronide conjugate of M4 [(3-{[[4-(2-hydroxy-1,1-dimethyl-ethyl)-

benzyl]-(pyridine-3-sulfonyl)-amino]-methyl}-phenoxy)-acetic acid glucuronide].

***Metabolite M14***.  M14 had a retention time of ~16.90 min on HPLC and was found only in bile.  It showed a protonated molecular ion at *m/z* 645, 176 amu higher than that of the parent drug, suggesting that it was a glucuronide conjugate.  The CID product ion spectrum of *m/z* 645 showed prominent fragment ions at *m/z* 469, 423, 413, 326, 165, and 147. The ion at *m/z* 469 occurred from loss of a glucuronic acid moiety from the molecule.  The other ions were similar to those observed for the parent drug.  Treatment of M14 with β-glucuronidase formed CP-533,536. Thus, M14 was tentatively identified as CP-533,536 glucuronide.

## Discussion

We here report the metabolic fate and disposition of CP-533,536 in SD rats. [$^{14}$C]CP-533,536 labeled at the benzylic carbon of the *tert*-butylphenyl ring was administered i.v. to male and female rats.  The administered radioactive dose was quantitatively recovered in both male (98%) and female (97%) rats.  The excretion of radioactivity was rapid, with 93.0% (male) and 92.4% (female) of the dose excreted within 24 h after drug administration.  The majority of the administered dose (>87%) was recovered in the feces in rats, providing indirect evidence of excretion *via* the bile.  There was no discernible gender difference in the excretion pattern of radioactivity in rats after i.v. administration of [$^{14}$C]CP-533,536.  However, pharmacokinetics and metabolism of CP-533,536 displayed distinct gender-related differences in male and female rats.  The elimination half-lives of CP-533,536 and total radioactivity in male and female rats were similar. But the plasma clearance of total radioactivity and unchanged drug were 1.5 to 2

"DMD #4713

fold higher in male rats compared to female rats.  Also the $VD_{ss}$ of parent drug

and total radioactivity was 2.6 to 3 fold higher in female rats than the male rats.

CP-533,536 was extensively metabolized.  Only 26% of the radioactive dose was

recovered as unchanged drug.  The remainder of the radioactivity was due to

Phase I and Phase II metabolites.  An overview of the metabolism pathways of

CP-533,536 is given in fig.11.  The major oxidative pathway was due to the

oxidation of the *tert*-butyl side chain to form the ω-hydroxy metabolite M4.  M4

was further oxidized to form the ω-carboxy metabolite M3 or conjugated with

sulfuric acid to form metabolite M6.  Other metabolites were due to N-oxidation of

the pyridine ring (M5), and hydroxylation and N-dealkylation of the methyl-

phenoxyacetic acid moiety followed by phase II conjugation.  In addition to the

parent drug, circulating metabolites included M4, M5 and M6.  Hydroxylation at

the tert-butyl side chain is not uncommon and, for example, was observed for

several drugs containing this side chain (Carlin et. al. 1997, Lin et. al., 2003).

The pathway leading to the formation of  the ω-carboxy metabolite involves the

formation of an aldehyde intermediate, which is then metabolized to the

carboxylic acid.  Although we were able to confirm the formation of an aldehyde

intermediate *in vitro* in human liver microsomes (unpublished data), we were not

able to detect this metabolite in *vivo*.

The metabolites were primarily characterized by the LC-MS/MS method, which is

clearly a technique of choice for the high-throughput and rapid structural

characterization of metabolites from biological fluids (Miao et al., 2001; Prakash et al., 1998; Johnson et al., 2003). Analysis of CID mass spectra of metabolites can easily distinguish oxidative possibilities when they occur in positions characterized by distinct product ions. However, the differentiation of N-oxide metabolite from C-hydroxylated metabolite can be difficult by mass spectrometry. We have earlier reported the use of $TiCl_3$ to prove the presence and absence of N-oxide functionality in the metabolites of the antipsychotic drug, ziprasidone (Prakash et al., 1997). Recently, this technique has been successfully used to selectively reduce N-oxides in the presence of sulfoxide and other labile groups (Kulanthaivel et al., 2004). We now employed this technique for the differentiation of three monooxygenated metabolites (M4, M5 and M12) of CP-533,536. The full scan LC-MS of metabolites, M4, M5 and M12 displayed protonated molecular ions at m/z 485, suggesting that these metabolites were monooxygenated and regioisomers. The fragment ions in the CID product ion spectra of M4 and M12 were able to define the site of oxidation at the *tert*-butyl side chain and phenoxy acetic acid moiety, respectively. However, as described for metabolite M5, the MS-MS spectrum did not provide adequate information to definitely establish of site of oxidation. The fragment ions at *m/z* 147, 165, and 326, similar to those obtained for the parent compound, suggested that the oxidation had occurred at the pyridine ring. In this case the definitive determination of oxidation at the nitrogen of the pyridine was confirmed by reduction of M5 with $TiCl_3$. Treatment of M5 with aqueous $TiCl_3$ resulted in the formation of parent compound, suggesting that M5 was an N-oxide. Therefore,

TiCl$_3$ reduction technique combine with MS proved useful for definitive structural characterization of isomeric metabolites.

Sex differences were apparent in the quantitative and qualitative nature of the excreted metabolites of CP-533,536. Metabolites M8 and M12 were only observed in male rats while M9 was detected in female rats. The relative amounts of metabolites in male plasma were higher than those in females, and the excretion ratios of metabolites to total radioactivity were higher in males than those of females. The occurrence of gender-related differences in drug metabolism, especially in the rat, has been reported for numerous drugs and occurs in both phase I and phase II metabolism (Maurizis et al., 1997; Nakagomi et al., 1997; Mugford and Kendderis 1998; Dix et al, 1999; Sato et al., 2000). One factor commonly known to contribute to gender-dependent metabolism is differential expression of drug metabolism enzymes, especially CYP isoforms (Mugford and Kendderis 1998). Female rats have 10-30% less total CYP 450 compared with male rats. Therefore, female rats, in general, have slower metabolism of many drugs than male rats. Our preliminary *in vitro* data using human liver microsomes suggest that the metabolism of CP-533,536 is mediated by CYP3A isozymes, which are preferentially expressed in male rats (Kobliakov et al., 1991). In contrast, females have higher expression of hydroxysteroid, glucocorticoid, and bile acid sulfotransferases (Mulder, 1986). We also observed that the sulfate conjugate M6 was formed in much higher quantities in female rats

than male rats suggesting that the sulfation of M3 may be mediated by a female specific sulfotransferase.

In conclusion, the results of this study provide the first analysis of formation and excretion of metabolites of CP-533,536 in rats, one of the species used in toxicology studies. CP-533,536 is metabolized in both male and female rats after i.v. administration and the radioactive dose is excreted mainly in feces via bile. CP-533,536 is eliminated by oxidation followed by conjugation. There were notable gender-related differences in pharmacokinetic and metabolic behavior in male and female rats. Finally, the identification of these metabolic pathways of CP-533,536 will aid in understanding its metabolism in humans.

**"DMD #4713**

**References**

Breyer RM, Bagdassarian CK, Myers SA and Breyer MD (2001). Prostanoid

Receptors: Subtypes and Signaling. *Annu Rev Pharmacol Toxicol* **41**:661-90.

Carlin JR, Christofalo P, Arison BH, Ellsworth RE, Rosegay A, Miller RR, Chiu

SHL and Nandenheuvel WJA (1997) Disposition and metabolism of finasteride in

dogs. *Drug Metab Dispos* **25:**100-109.

Dix KJ, Coleman DP, and Jeffcoat AR (1999) Comparative metabolism and

disposition of gemfibrozil in male and female Sprague-Dawley rats and Syrian

golden hamsters. *Drug Metab Dispos* **27:**138-146.

Jee, WS and Ma YF (1997) The in vivo anabolic actions of prostaglandins in

bone. *Bone* **21:**297-304.

Johnson K, Prakash C, Shah A, Jaw J and Baxter J (2003) Metabolism,

pharmacokinetics, and excretion of a highly selective NMDA receptor antagonist,

traxoprodil, in human cytochrome P450 2D6 extensive and poor metabolizers.

*Drug Metab Dispos* **31:**76-87.

Ke  HZ, Shen VW, Qi H, Crawford DT, Wu DD, Liang XG, Chdsey-Frink KL, Pine

CM, Simmons HA, Thompson DD (1998) Prostaglandin E2 increases bone

"DMD #4713

strength in intact rats and in ovariectomized rats with established osteopenia *Bone* **23**:249-255.

Kobliakov V, Popovaand N and Rossi L. (1991)  Regulation of the expression of the sex-specific isoforms of cytochrome P450 in rat liver. *Eur J Biochem* **195**: 585-591.

Kulanthiaivel P, Barbuch RJ, Davidson RS, Yi P, Rener GA, Mattiuz EL, Hadden CE, Goodwin LA and Ehlhardt WJ (2004) Selective reduction of N-oxides to amines: application to drug metabolism. *Drug Metab Dispos* **32:**966-972.

Lin J, Colizza K, and Prakash C. (2003) Characterization of the unusual C-demethylated metabolites of the NK1 receptor antagonist, CJ-11,972, in human liver microsomes and 3A isoforms by LC-MS/MS. ASMS Conference on Mass Spectrometry and Allied Topics. Montreal, Canada.

Maurizis JC, Madelmont JC, Rapp M, Marijnen C, Cerf MC, Gillardin JM, Lepage F and Veyre A (1997) Disposition and metabolism of 2,6-dimethylbenzamide N-(5-methyl-3-isoxazoleyl) (D2916 in male and female rats. *Drug Metab Dispos* **25:**33-39.

Melton LJ III. Epidemiology of Fractures. In: Riggs BL, Melton LJ III, editors.

Osteoporosis: Etiology, Diagnosis and Management. 2nd Ed. Philadelphia:

Lippincott-Raven Press; 1995. p. 225-47.


Miao Z, Lawrence J, Janisweki J and Prakash C (2000) Rapid identification of the

major *in vitro* metabolites of new chemical entities using 96 well plate solid phase

extraction and ion trap mass spectrometry. 47th ASMS Conference on Mass

Spectrometry and Allied Topics. Dallas, TX.


Mugford CA and Kedderis GR (1998) Sex-dependent metabolism of xenobiotics.
*Drug Metab Rev* **30:**441-498.


Mulder G (1986) Sex differences in drug conjugation and their consequences for

drug toxicity. Sulfation, glucuronidation and glutathione conjugation.
*Chem Biol Interact* **57**:1-15.


Nakagomi M, Suzuki E, Kitashima M, Iida S, Abe M, Matsuki Y and Kaneko K

(1997) Sex difference in the metabolism of pirmenol in rats. *Biol Pharm Bull* **20**

**(12):**1279-1284.


Paralkar VM, Borovecki F, Ke HZ, Cameron KO, Lefker B, Grasser WA, Owen

TA, Li M, Dasilva-Jardine P, Zhou M, Dunn RL, Dumont F, Korsmeyer R,

Krasney P, Brown TA, Plowchalk D, Vukicevic S and Thompson DD (2003). An

EP2 receptor-selective prostaglandin E$_2$ agonist induces bone healing. *Proc Nat Acad Sci* **100**: 6736-6740.

Prakash, C., Kamel, A, and Cui D. (1997) Characterization of the novel benzisothiazole ring cleaved products of the antipsychotic drug, ziprasidone. *Drug Metab. Dispos.* **25**: 897-901.

Prakash C, Cui D, Bright GM, Baxter J, Miceli J and Wilner K (1998) Metabolism and excretion of a new anxiolytic drug candidate, CP-93,393, in healthy male volunteers. *Drug Metab Disp* **26:**448-456.

Sato M, Suzaka H and Miazaki H (2000) Sex-related differences in urinary excretion of egualen sodium in rats. *Drug Matab Dispos* **28:**21-27.

**"DMD #4713**

**Footnotes:**

Send reprints requests to: Chandra Prakash, Ph. D., Department of Pharmacokinetics, Dynamics and Metabolism, Pfizer Global Research and Development, Groton, CT 06340. Ph. No. 860-441-6415. Fax No. 860-441-4109

This work was presented in part at the 4th American Society of Mass Spectrometry and Allied Topics. Chicago, IL, 2001.

**"DMD #4713**

**Figure Legends:**

FIG. 1. The structure of CP-533,536 in rats (* denotes the position of ^{14}C-label)

Fig. 2. Plasma concentration time curves of unchanged CP-533,536 and total radioactivity in male and female rats after a single 15 mg/kg i.v. dose of [^{14}C]CP-533,536

FIG. 3. HPLC-radiochromatograms of CP-533,536 metabolites in urine of male and female rats after a single 15 mg/kg i.v. dose of [^{14}C]CP-533,536

FIG. 4. HPLC-radiochromatograms of CP-533,536 metabolites in feces of male and female rats after a single 15 mg/kg i.v. dose of [^{14}C]CP-533,536

FIG. 5. HPLC-radiochromatograms of CP-533,536 metabolites in bile of male and female rats after a single 15 mg/kg i.v. dose of [^{14}C]CP-533,536

FIG. 6. HPLC-radiochromatograms of CP-533,536 metabolites in plasma of (A) male (4 h) and (b) female (4 h) rats after a single 15 mg/kg i.v. dose of [^{14}C]CP-533,536

FIG. 7. CID product ion mass spectrum of CP-533,536

FIG. 8. CID product ion spectrum of metabolite M4 (*m/z* 485)

**"DMD #4713**

FIG. 9.  CID product ion spectrum of metabolite M5 (*m/z* 485)

FIG. 10.  CID product ion spectrum of metabolite M12 (*m/z* 485)

FIG. 11. Proposed biotransformation pathways of CP-533,536 in rats

Table 1. Percentage (mean±SD) of dose excreted in urine and feces from rats following i.v. administration of [$^{14}$C]CP-533,536

| Collection Time (h) | Male Rats (N=3) | | | Female Rats (N=3) | | |
|---|---|---|---|---|---|---|
| | Urine | Feces | Total | Urine | Feces | Total |
| 0-24 | 10.8±3.08 | 82.2±2.21 | 93.0±1.01 | 8.27±1.22 | 84.1±4.46 | 92.4±5.65 |
| 24-48 | 0.80±0.27 | 3.55±1.82 | 4.36±2.08 | 0.64±0.23 | 3.31±1.90 | 3.95±1.69 |
| 48-72 | 0.20±0.12 | 0.27±0.16 | 0.47±0.28 | 0.11±0.03 | 0.20±0.12 | 0.31±0.09 |
| 72-96 | 0.06±0.03 | 0.06±0.01 | 0.12±0.03 | 0.07±0.06 | 0.05±0.02 | 0.12±0.07 |
| 96-120 | 0.06±0.05 | 0.09±0.06 | 0.16±0.10 | 0.04±0.01 | 0.10±0.03 | 0.14±0.04 |
| 120-144 | 0.06±0.04 | 0.03±0.01 | 0.09±0.05 | 0.05±0.01 | 0.06±0.03 | 0.11±0.02 |
| 0-144 | 12.0±3.41 | 86.2±1.33 | 98.2±3.44 | 9.18±1.31 | 87.8±3.58 | 97.0±4.82 |

Table 2.  Pharmacokinetic parameters for CP-533,536 and total radioactivity

| Analyte | Sex[a] | $C^{bc}$ (µg/ml) | $VD_{ss}$ (l/kg) | $AUC_{0-\infty}{}^{d}$ (µg•hr/ml) | $Cl_p$ (ml/min/kg) |
|---|---|---|---|---|---|
| CP-533,536 | Male | 20.0±6.47 | 2.93±1.71 | 9.72±2.80 | 30.2±13.9 |
| | Female | 33.1±8.76 | 0.71±0.19 | 15.6±0.82 | 16.1±0.8 |
| Total | Male | 20.1±8.65 | 5.93±3.98 | 15.5±4.44 | 17.3±5.9 |
| Radioactivity | Female | 34.5±5.65 | 2.37±1.36 | 21.5±4.33 | 11.9±2.2 |

[a] N=3/gender

[b] Plasma concentrations are reported for first time point (15 min) after

administration

[c] Plasma concentration for radioactivity is reported in µg-equiv/ml.

[d] $AUC_{0-\infty}$ for radioactivity is reported in µg-equiv•h/ml.

Table 3. Percentages of the administered (mean±SD) of urinary and fecal

metabolites of CP-533,536 in male and female rats following i.v. administration of

[$^{14}$C]CP-533,536.

| Metabolite (#) | Retention Time (min:sec) | Males | | | Female | | |
|---|---|---|---|---|---|---|---|
| | | Urine | Feces | Total | Urine | Feces | Total |
| M8 | 11:35 | 2.22±0.99 | - | 2.22±0.99 | - | - | - |
| M9 | 11:35 | - | - | - | 0.62±0.06 | - | 0.62±0.06 |
| M11 | 14:20 | 5.66±2.56 | - | 5.66±2.56 | 1.59±1.59 | - | 1.59±1.59 |
| M6 | 12:37 | - | 12.7±4.18 | 12.7±4.18 | - | 36.2±5.05 | 36.2±5.05 |
| M10 | 13:26 | - | 1.05±0.12 | 1.05±0.12 | 4.95±0.90 | 7.34±3.26 | 12.3±4.16 |
| M3 | 14:21 | - | 32.8±6.72 | 32.8±6.72 | - | 1.66±0.78 | 1.66±0.78 |
| M4 | 14:49 | - | 19.7±0.58 | 19.7±0.58 | 0.88±0.09 | 5.64±1.17 | 6.52±1.26 |
| M12 | 17:50 | - | 1.39±0.22 | 1.39±0.22 | - | - | - |
| Parent | 19:17 | - | 16.2±2.86 | 16.2±2.86 | - | 35.6±4.85 | 35.6±4.85 |

Table 4. Average percentages of total radioactivity of biliary and circulating

metabolites of CP-533,536 in male and female rats following i.v. administration of

[$^{14}$C]CP-533,536.

| Metabolite # | Retention Time (min:sec) | Male | | | Female | | |
|---|---|---|---|---|---|---|---|
| | | Bile | Plasma 1h | Plasma 4h | Bile | Plasma 1h | Plasma 4h |
| M8 | 11:35 | 3.55 | | | 1.2 | | |
| M13 | 10:47 | 2.5 | | | - | | |
| M11 | 14:20 | 1.6 | | | 2.45 | | |
| M6 | 12:37 | 10.3 | 9.27 | 7.17 | 22.6 | - | 2.65 |
| M10 | 13:26 | | | | | | |
| M3 | 14:21 | 7.3 | | | | | |
| M4 | 14:49 | 8.5 | 27.1 | 25.6 | 1.4 | 6.27 | 15.9 |
| M5 | 15:23 | 9.5 | 10.9 | 46.1 | 2.2 | 1.75 | 16.0 |
| M12 | 17:50 | 2.15 | | | * | | |
| M14 | 16:90 | * | | | * | | |
| Parent | 19:17 | 53.9 | 34.0 | 21.1 | 70.1 | 90.3 | 65.4 |

* Metabolites were observed by LC/MS but not able to be quantitated by
Radioactivity

**"DMD #4713**

Table 5.  Major CID product ions of metabolites of CP-533,536

| Metabolite | M+H$^+$ | Major CID Fragment Ions (*m/z*) |
|---|---|---|
| CP-533,536 | 469 | 423 (MH-HCOOH), 413, 326,165,147 |
| M3 | 499 | 453 (MH-HCOOH), 356, 310, 165,131 |
| M4 | 485 | 467 (MH-H$_2$O), 342, 324, 165,145 |
| M5 | 485 | 439 (MH-HCOOH), 429, 326, 165,147 |
| M6 | 565 | 485 (MH-SO$_3$), 467, 342, 324, 165,145 |
| M8 | 351 | 305 (MH-HCOOH), 146,131 |
| M9 | 417 | 319 (MH-H$_2$SO$_4$), 160, 145 |
| M10 | 401 | 303 (MH-H$_2$SO$_4$), 160,145 |
| M11 | 335 | 289 (MH-HCOOH), 146, 131 |
| M12 | 485 | 342, 305, 181, 162,147 |
| M13 | 661 | 485 (MH-Glu), 467, 342, 324, 165,145 |
| M14 | 645 | 469 (MH-Glu), 423, 413, 326,165,147 |
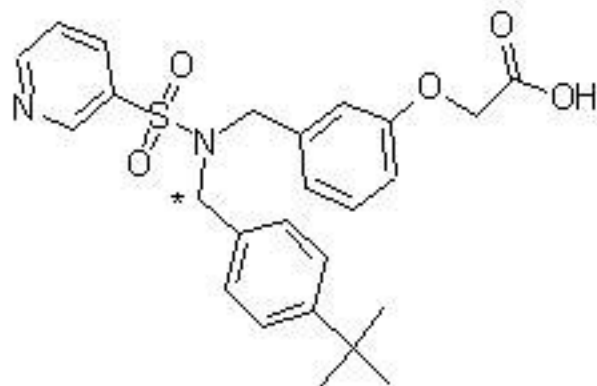
* Denotes the position of $^{14}$C-label

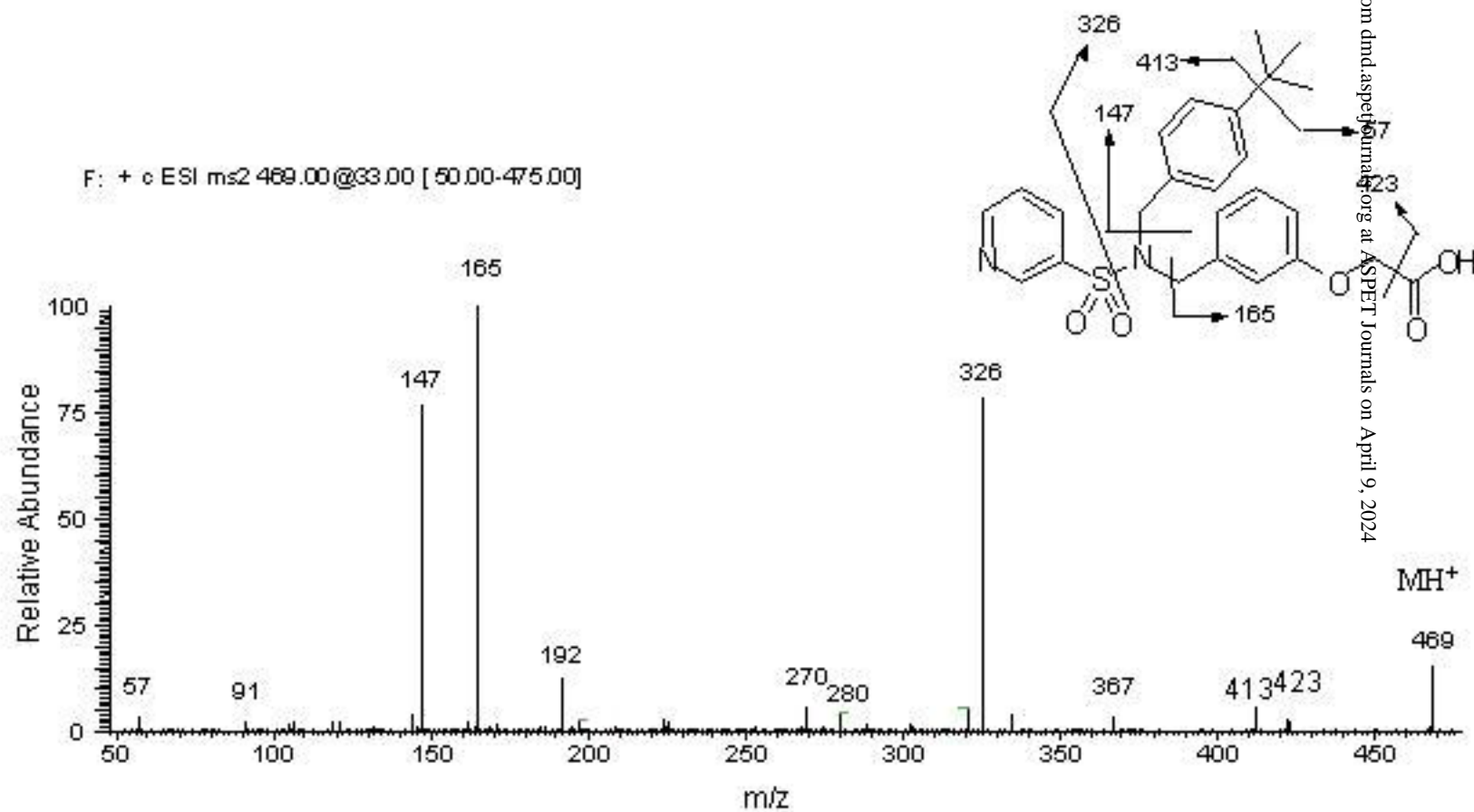Fig. 1.
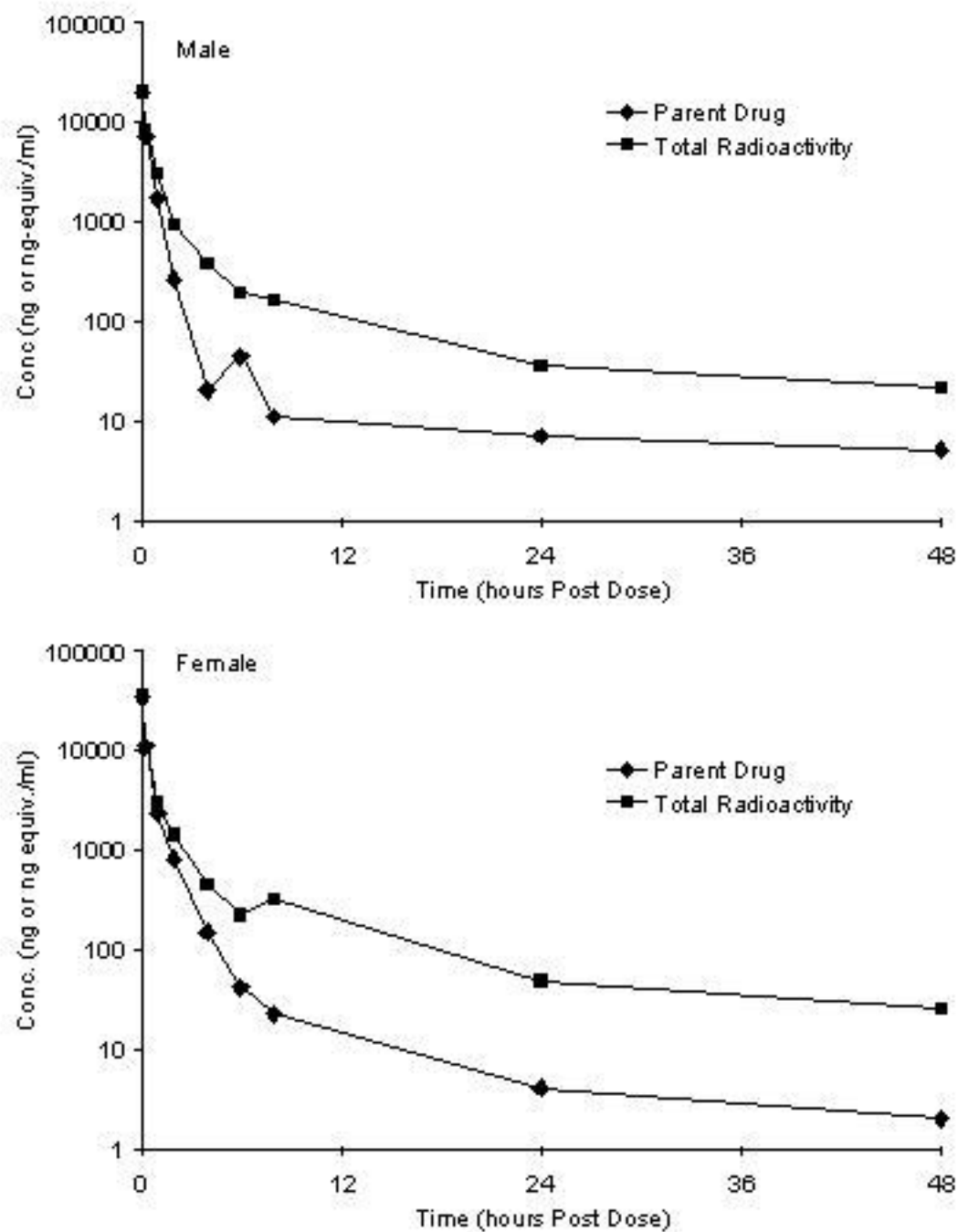
Fig 2

FIG. 3.

FIG. 4.
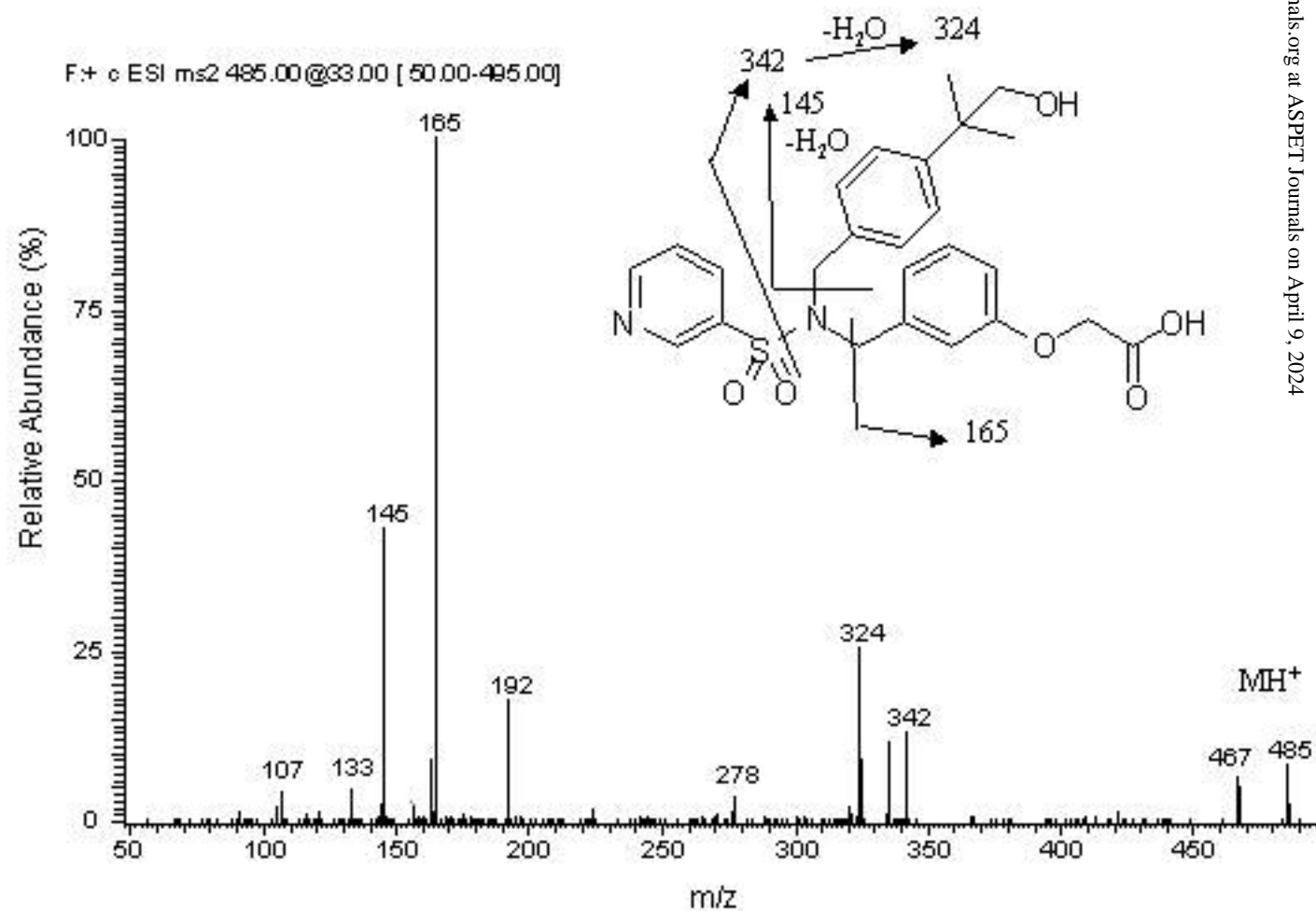
FIG. 5.

FIG. 6.

F: + c ESI ms2 469.00@33.00 [ 50.00-475.00]
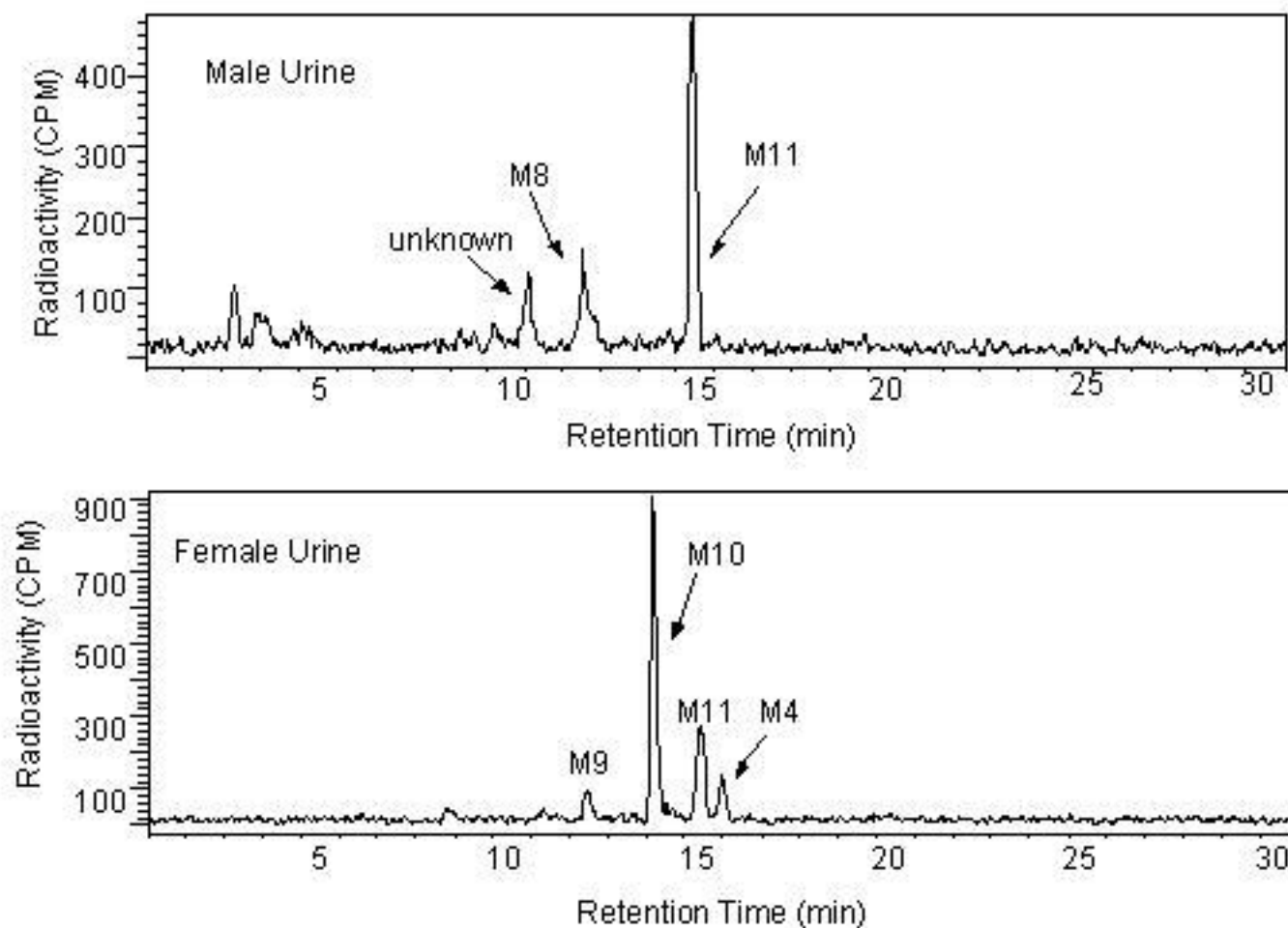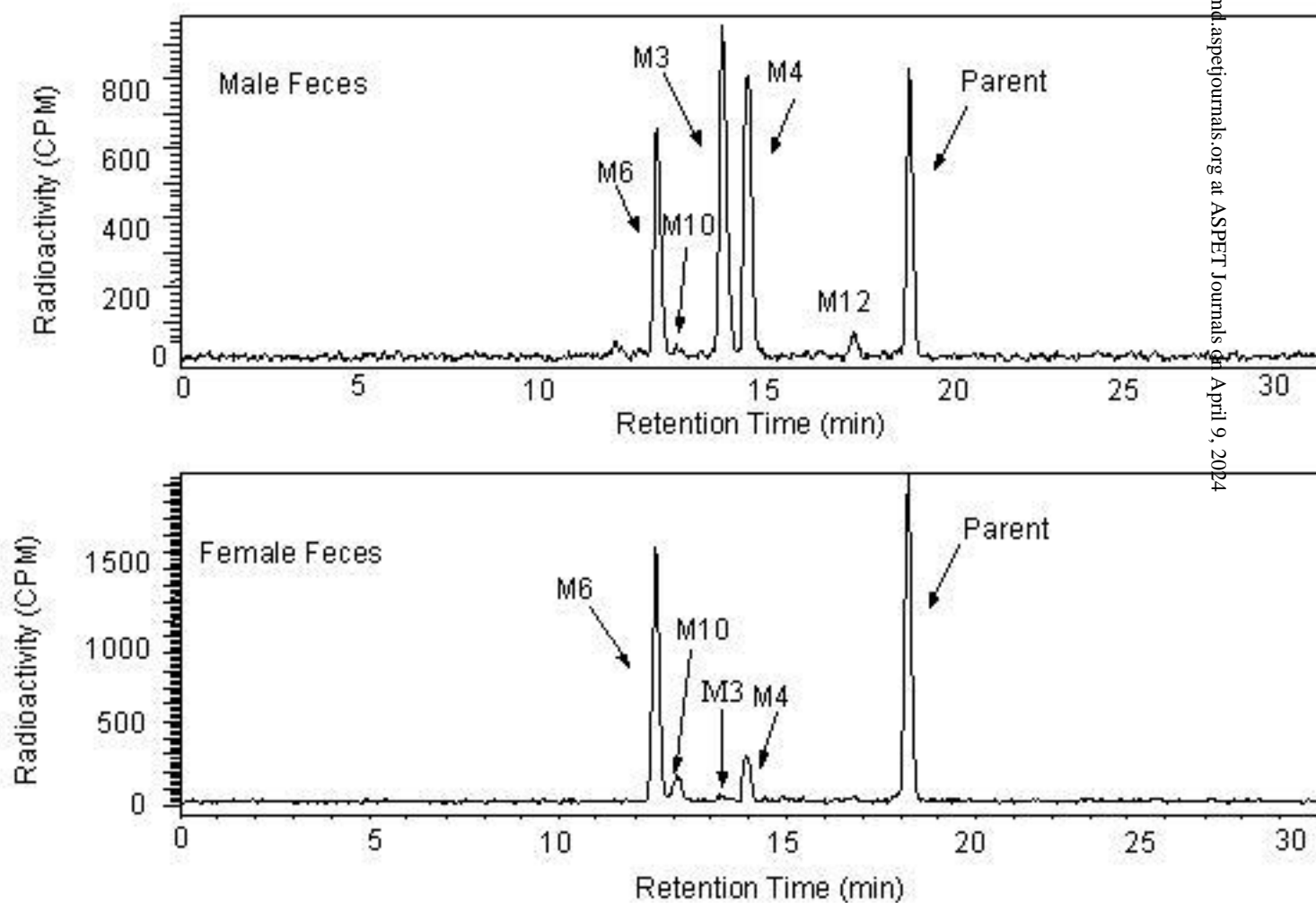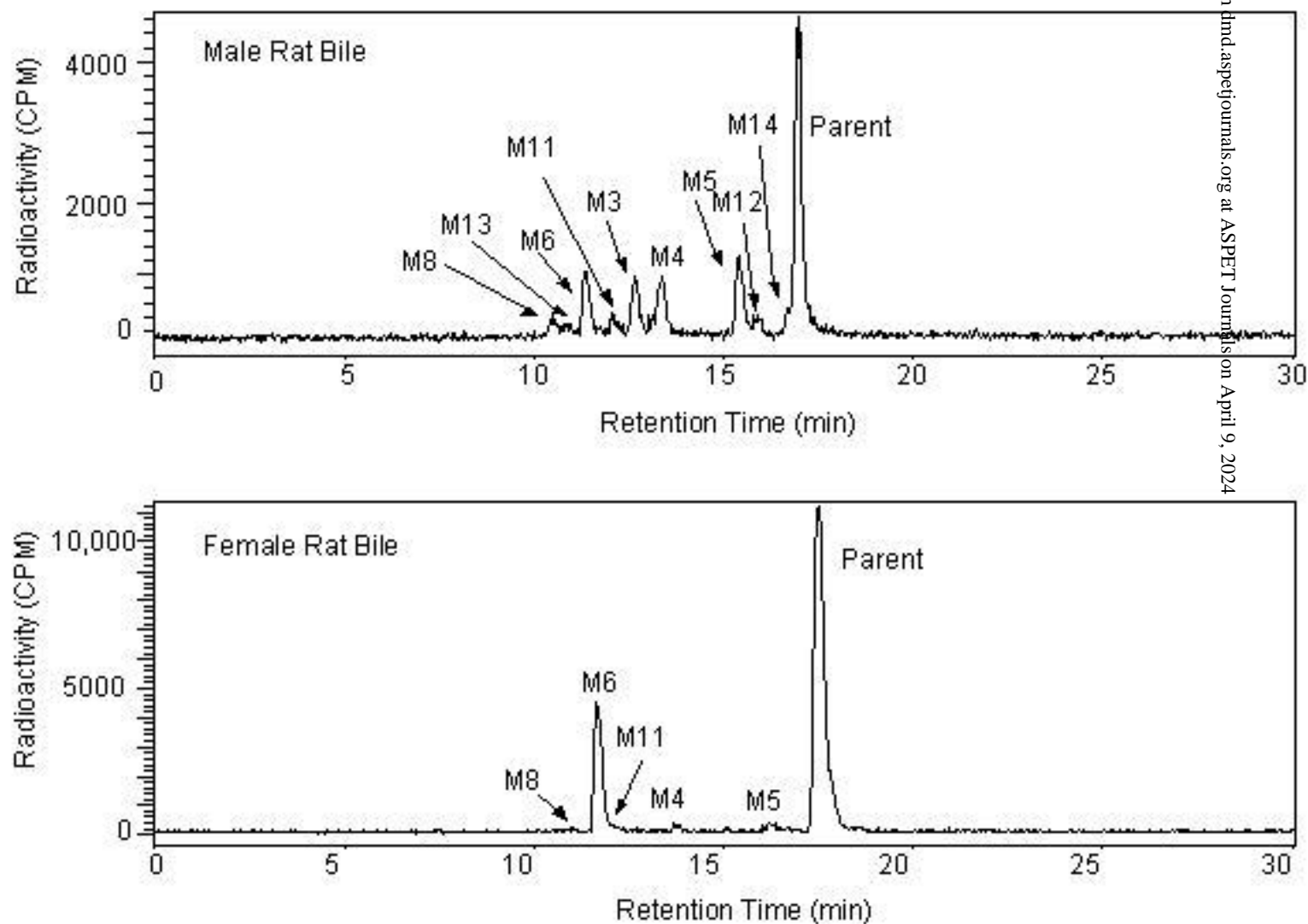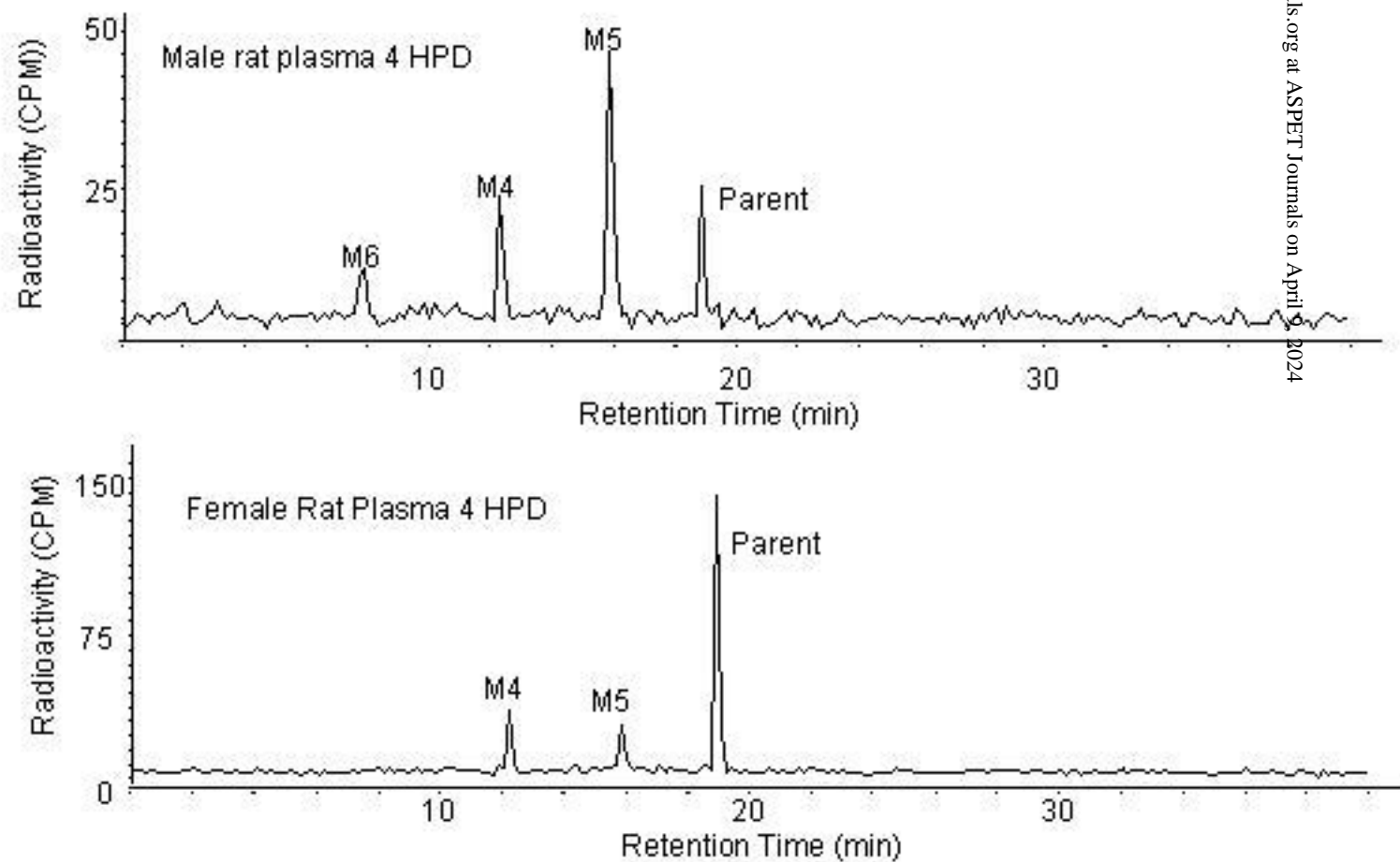


FIG. 7.

FIG. 8.

FIG. 9.

FIG. 10.

FIG. 11